

## Conduction mechanisms in p-type $\text{Pb}_{1-x}\text{Eu}_x\text{Te}$ alloys in the insulator regime

M. L. Peres, R. M. Rubinger, L. H. Ribeiro, C. P. L. Rubinger, G. M. Ribeiro et al.

Citation: *J. Appl. Phys.* **111**, 123708 (2012); doi: 10.1063/1.4729813

View online: <http://dx.doi.org/10.1063/1.4729813>

View Table of Contents: <http://jap.aip.org/resource/1/JAPIAU/v111/i12>

Published by the [American Institute of Physics](#).

---

### Related Articles

Laser induced thermal-wave fields in multi-layered spherical solids based on Green function method  
*J. Appl. Phys.* **112**, 033521 (2012)

Influence of the magnetic field on the plasmonic properties of transparent Ni anti-dot arrays  
*Appl. Phys. Lett.* **101**, 063107 (2012)

Large half-metallic gap in ferromagnetic semi-Heusler alloys CoCrP and CoCrAs  
*Appl. Phys. Lett.* **101**, 062402 (2012)

The Curie temperature distribution of FePt granular magnetic recording media  
*Appl. Phys. Lett.* **101**, 052406 (2012)

Micro-dent arrays fabricated by a novel net mask laser shock processing on the surface of LY2 aluminum alloy  
*J. Appl. Phys.* **112**, 023117 (2012)

---

### Additional information on J. Appl. Phys.

Journal Homepage: <http://jap.aip.org/>

Journal Information: [http://jap.aip.org/about/about\\_the\\_journal](http://jap.aip.org/about/about_the_journal)

Top downloads: [http://jap.aip.org/features/most\\_downloaded](http://jap.aip.org/features/most_downloaded)

Information for Authors: <http://jap.aip.org/authors>

## ADVERTISEMENT

**World's Ultimate AFM** Experience the Speed & Resolution



**The fastest AFM on the planet is now simply the best AFM in the world**

[CLICK TO REQUEST INFO](#)

**Conduction mechanisms in  $p$ -type  $\text{Pb}_{1-x}\text{Eu}_x\text{Te}$  alloys in the insulator regime**M. L. Peres,<sup>1,a)</sup> R. M. Rubinger,<sup>1</sup> L. H. Ribeiro,<sup>1</sup> C. P. L. Rubinger,<sup>1</sup> G. M. Ribeiro,<sup>2</sup> V. A. Chitta,<sup>3</sup> P. H. O. Rappl,<sup>4</sup> and E. Abramof<sup>4</sup><sup>1</sup>*Departamento de Física e Química, Instituto de Ciências Exatas, Universidade Federal de Itajubá, Itajubá, PB 50, MG CEP 37500-903, Brazil*<sup>2</sup>*Departamento de Física, ICEx, Universidade Federal de Minas Gerais, Belo Horizonte, PB 702, MG CEP 30123-970, Brazil*<sup>3</sup>*Instituto de Física, Universidade de São Paulo, São Paulo, PB 66318, SP CEP 05315-970, Brazil*<sup>4</sup>*Laboratório Associado de Sensores e Materiais, Instituto Nacional de Pesquisas Espaciais, São José dos Campos, PB 515, SP CEP 12201-970, Brazil*

(Received 28 March 2012; accepted 16 May 2012; published online 19 June 2012)

Electrical resistivity measurements were performed on  $p$ -type  $\text{Pb}_{1-x}\text{Eu}_x\text{Te}$  films with Eu content  $x = 4\%$ ,  $5\%$ ,  $6\%$ ,  $8\%$ , and  $9\%$ . The well-known metal-insulator transition that occurs around  $5\%$  at room temperature due to the introduction of Eu is observed, and we used the differential activation energy method to study the conduction mechanisms present in these samples. In the insulator regime ( $x > 6\%$ ), we found that band conduction is the dominating conduction mechanism for high temperatures with carriers excitation between the valence band and the  $4f$  levels originated from the Eu atoms. We also verified that mix conduction dominates the low temperatures region. Samples with  $x = 4\%$  and  $5\%$  present a temperature dependent metal insulator transition and we found that this dependence can be related to the relation between the thermal energy  $k_B T$  and the activation energy  $\Delta\varepsilon_a$ . The physical description obtained through the activation energy analysis gives a new insight about the conduction mechanisms in insulating  $p$ -type  $\text{Pb}_{1-x}\text{Eu}_x\text{Te}$  films and also shed some light over the influence of the  $4f$  levels on the transport process in the insulator region. © 2012 American Institute of Physics.

[<http://dx.doi.org/10.1063/1.4729813>]

**I. INTRODUCTION**

The  $\text{Pb}_{1-x}\text{Eu}_x\text{Te}$  is a IV–VI semiconductor alloy that has been applied on the fabrication of mid infrared sensors and diode lasers<sup>1,2</sup> due to the large tunability of the energy gap with variation of Eu content. It also presents very interesting physical properties that differs it from the other more commonly studied semiconductors: the introduction of  $\text{Eu}^{2+}$  ions to form the  $\text{Pb}_{1-x}\text{Eu}_x\text{Te}$  alloy drastically changes the optical and electrical properties of this semiconductor.<sup>3</sup> The energy gap located at the  $L$  point of the Brillouin zone increases, while the carrier mobility is reduced, as the Eu content is augmented. Also, the increasing of the Eu content  $x$  leads to a metal-insulator transition that occurs around  $x = 5\%$  for  $p$ -type samples<sup>3</sup> and around  $x = 10\%$  for  $n$ -type samples.<sup>4</sup> The transition occurs due the disorder caused by the Eu atoms and it is an Anderson transition type.

Another important consequence of the introduction of the Eu ions is the formation of the  $4f$  level below the valence band maximum for  $x < 6\%$ .<sup>5</sup> For  $x = 6\%$ , the  $4f$  level broadens with the valence band maximum and for  $x > 6\%$  the  $4f$  levels penetrates the energy gap.<sup>6</sup> Through optical measurements, Krenn *et al.*<sup>6</sup> verified that in this situation the original transitions between the  $L^+_6$  and  $L^-_6$  points (valence and conduction band respectively) changes to transitions between the  $4f$  states and the  $L^-_6$ . Regarding to the electrical properties, the influence of the  $4f$  states for  $x > 6\%$  on the transport

process is not clear. Despite the strong localization of the  $4f$  core levels, there are indications that these states indeed alter some electrical properties.<sup>3</sup>

In this work, we performed electrical resistance measurements on  $p$ -type  $\text{Pb}_{1-x}\text{Eu}_x\text{Te}$  samples with  $x = 4\%$ ,  $5\%$ ,  $6\%$ ,  $8\%$ , and  $9\%$ . From the analysis of the experimental curves using the differential activation energy (DAE) method,<sup>7</sup> we investigated the conduction mechanisms present in the samples. Through the DAE curves obtained from the experimental data, we found that the band conduction dominates at higher temperatures for samples with  $x = 8\%$  and  $9\%$ . For samples with  $x = 4\%$ ,  $5\%$ , and  $6\%$ , it is possible to identify a mix conduction, indicating that these samples are in a transition region where more than one mechanism plays an important role, i.e., it is possible that the diffusive regime coexists with the thermally activated or hopping regimes. We also compared the activation energies  $\Delta\varepsilon_a$  to the thermal energy  $k_B T$  and found that the reduction or saturation of the electrical resistance observed in some samples at low temperatures can be related to the relation between  $\Delta\varepsilon_a$  and  $k_B T$ . Recently, new methods of gating and nanostructure fabrication of  $\text{PbTe}/\text{Pb}_{1-x}\text{Eu}_x\text{Te}$  quantum wells were suggested for possible application of this material on spintronic based devices.<sup>8–10</sup> Hence, we expect that the detailed description of the conduction mechanisms and the influence of the  $4f$  levels on them can lead to improvements on the application of  $\text{PbEuTe}$  alloys on electrical and optical devices as well as in the development of spintronic devices that could be designed to operate in a given temperature range.

<sup>a)</sup>E-mail: marcelos@unifei.edu.br.

## II. EXPERIMENTAL

The measurements were performed on films of *p*-type  $\text{Pb}_{1-x}\text{Eu}_x\text{Te}$  with  $x$  varying from 4% up to 9%. The samples were grown in a Riber 32P molecular-beam epitaxy MBE system onto freshly cleaved (111)  $\text{BaF}_2$  substrates. The films were grown at a substrate temperature of 208.5 °C during 2 h, with a deposition rate of 3.9 Å/s, resulting in a 2.8 μm layer thickness. Three effusion cells with PbTe, Eu, and  $\text{Te}_2$  were used to grow the samples. Pb (Te) vacancies in PbTe crystals act as acceptors (donors); therefore, it is possible to control the concentration and the type of carriers through the chalcogen source flux variation. To provide a *p*-type sample, an excess of  $\text{Te}_2$  was maintained during the growth. The flux rates from the individual effusion cells were measured with an ion gauge, which is mounted on the sample manipulator and can be rotated to the substrate growth position. To obtain crystals with different Eu contents, the ratio between the PbTe and Eu flux rates was varied.

## III. RESULTS AND DISCUSSION

Figure 1 presents the normalized electrical resistance ( $R_N$ ) for *p*-type  $\text{Pb}_{1-x}\text{Eu}_x\text{Te}$  samples as a function of the temperature in the range of 5–400 K and for  $x = 4\%$ , 5%, 6%, 8%, and 9%. Through this figure, it is possible to observe that a metal-insulator transition occurs around 5%, which is in agreement to previous results reported in literature.<sup>3</sup> This transition is caused by the disorder originated from the Eu ions, and the higher is the Eu content, deeper in the insulator side lays the sample. For high temperatures ( $T > 200$  K), the metal-insulator transition is clearly observed as the curves change the slope signal when  $x$  varies from 4% to 9%. However, samples with  $x = 4\%$  and 5% (see inset to better visualize the 5% sample profile) are considered to be in a transition region, i.e., both present metallic and insulator behaviors depending on the temperature region and tend to saturate as temperatures reached the minimum value measured here. In addition, the sample with  $x = 8\%$  exhibited

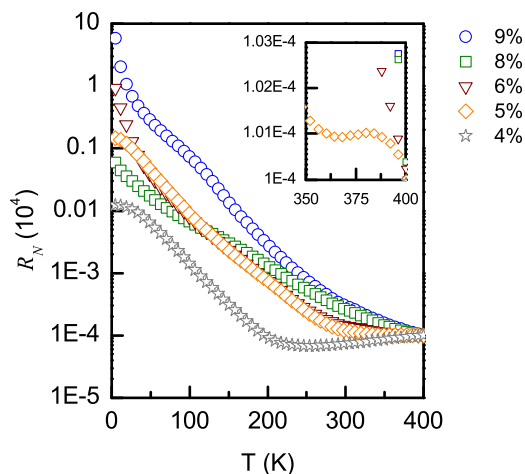


FIG. 1. Normalized electrical resistance ( $R_N$ ) for *p*-type  $\text{Pb}_{1-x}\text{Eu}_x\text{Te}$  samples as a function of the temperature in the range of 5–400 K and for  $x = 4\%$ , 5%, 6%, 8%, and 9%. The metal-insulator transition occurs around 5%. The inset shows the profile for the 5% sample that exhibits a metal-insulator transition as the temperature decreases.

electrical resistance values only higher than the sample with  $x = 4\%$  and lower than all the others as the temperatures decreased below  $\sim 130$  K.

In order to investigate the conduction mechanisms in the insulating samples, we performed an analysis using the DAE method.<sup>7</sup> This method allows one to obtain the activation energies involved in the carrier transport in a non-diffusive regime. The method consists in obtaining the activation energies from a numerical derivation of natural logarithm of the electrical resistance curves  $\left(\frac{d(\ln R)}{d(k_B T)^{-1}}\right)$  as a function of  $(k_B T)^{-1}$ . The temperature dependence of DAE is a good method to distinguish between variable range hopping (VRH), nearest neighbor hopping (NNH), or band conduction (Arrhenius) because the last two do not present temperature dependence. Hence, if the band conduction, i.e.,  $(\exp(hv/k_B T))$ , and NNH, i.e.,  $(\exp(hv'/k_B T))$ , regimes are present, where  $hv$  and  $hv'$  are constants,<sup>11</sup> the resulting activation energies obtained from the numerical derivation must be constants. Hence in Figure 2, we present the activation energy values as a function of temperature obtained from the electrical resistance curves presented in Figure 1. One can observe that samples with  $x = 8\%$  and 9% presented plateaus in the high temperature region indicating that band conduction dominates for such temperatures. The observed negative activation energy values for the sample with  $x = 4\%$  comes from the metallic character of this sample and, as the temperatures decreases, the energy increases until a maximum and changes slope around 177 K. The inversion of slope as the temperature decreases is also observed for samples with  $x = 5\%$ , and 6% and indicates that these samples are in the transition region. This reveals that, even though the resistance curve for the sample with  $x = 6\%$  presented insulator like behavior in the whole range of temperatures measured,

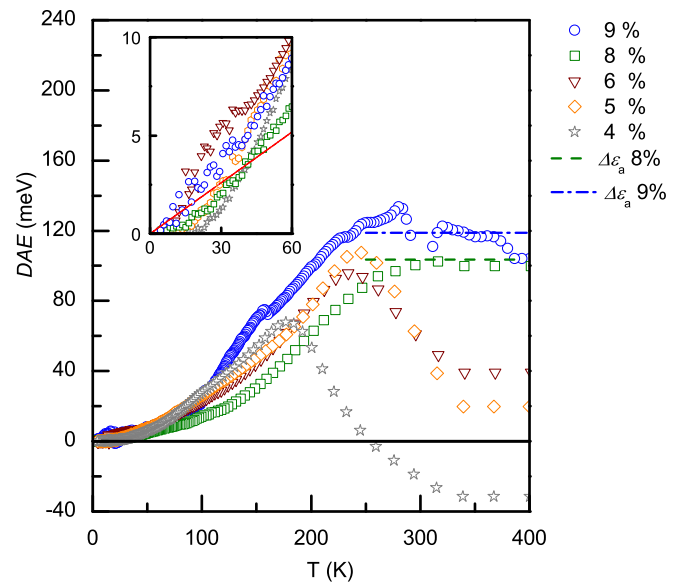


FIG. 2. Activation energy values as a function of temperature obtained from the electrical resistance curves presented in Figure 1. Samples with  $x = 8\%$  and 9% presented plateaus in the high temperature region indicating that band conduction dominates while the negative activation energy values for the sample with  $x = 4\%$  comes from the metallic character of this sample. (See text for further explanation.)

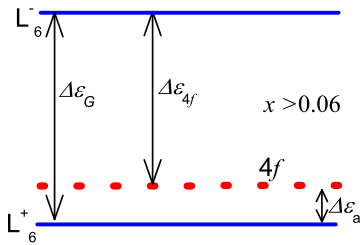


FIG. 3. Pictorial description of the position of the  $4f$  level with respect to the valence ( $L_6^+$ ) and band conduction ( $L_6^-$ ) and the energies  $\Delta\varepsilon_G(x)$ ,  $\Delta\varepsilon_{4f}(x)$ ,  $\Delta\varepsilon_a(x)$ . The calculated values for  $\Delta\varepsilon_a(x)$  are very close with those obtained from the plateaus observed in Figure 2 for samples with  $x=8\%$  and  $9\%$ .

this sample is not entirely insulating. Furthermore, at low temperatures, for  $T < 40$  K, it is possible to observe through the inset in Figure 2 that the activation energies for the samples with  $x=4\%$ ,  $5\%$ , and  $8\%$  drops below the thermal energy (full line), while the ones for samples with  $x=6\%$  and  $9\%$  remains above it until the lowest temperature measured. This is an indication that the thermal energy could play an important role even at low temperatures, i.e., hole carriers could be thermally activated from a region of localized states to a region of delocalized states leading to a reduction of electrical resistance. This could explain the resistance saturation observed for samples with  $x=4\%$  and  $5\%$  and the reduction of resistance for sample with  $x=8\%$  at low temperatures. In addition, all samples present a decrease of the activation energy as the temperature decreases after a certain value. In this temperature region, it is not possible to identify a dominating conduction regime and we indicate this region as dominated by a mix conduction regime.

The values of the activation energy obtained at high temperatures from the plateaus for samples with  $x=8\%$  and  $9\%$  indicate that must there be an energy level which separation from the valence band is smaller than the energy gap. The energy gap  $\Delta\varepsilon_G$  for  $\text{Pb}_{1-x}\text{Eu}_x\text{Te}$  samples with  $x=8\%$  and  $9\%$  are expected to be around 606 meV and 641 meV, respectively, using the equation given in Ref. 12 and nearly constant between 300 K and 400 K. These values show that, in fact, the carriers activation is not between valence and band conduction, i.e., between  $L_6^+$  and  $L_6^-$  points. However, as told before, the  $4f$  level forms a band that penetrates the energy gap for  $x > 6\%$  and, according to Krenn *et al.*,<sup>6</sup> the energy gap value, taking the  $4f$  level as the initial state of the interband transitions, can be calculated using  $\Delta\varepsilon_{4f}(x) = (0.34 + 2.03 \times x)$  which leads to the values of 502 meV and 523 meV for  $x=8\%$  and  $9\%$ , respectively. Considering that the carriers activation occurs between the  $L_6^+$  point and the  $4f$  band (empty states in the top of the  $4f$  band), we calculated the activation energy as  $\Delta\varepsilon_a(x) = \Delta\varepsilon_G - \Delta\varepsilon_{4f}(x)$  and obtained the value of 104 meV for  $x=8\%$  and 118 meV for  $x=9\%$ . These values are indicated in Figure 2 as dashed lines and are in good agreement to the values obtained through the DAE method since the dashed lines lays approximately in the plateaus. In Figure 3, we indicate the position of the  $4f$  level with respect to the

valence ( $L_6^+$ ) and band conduction ( $L_6^-$ ) and show the energies  $\Delta\varepsilon_G(x)$ ,  $\Delta\varepsilon_{4f}(x)$ ,  $\Delta\varepsilon_a(x)$ . This figure presents a simplified representation of the activation energy mechanism discussed above.

#### IV. CONCLUSIONS

We have measured electrical resistance on  $p$ -type  $\text{Pb}_{1-x}\text{Eu}_x\text{Te}$  samples for  $x=4\%$ ,  $5\%$ ,  $6\%$ ,  $8\%$ , and  $9\%$  and, using the activation energy method, we identified band and mixed conduction mechanisms in very precise temperatures regions between 5 up to 400 K. We found that for high Eu concentrations ( $x=8\%$  and  $9\%$ ), band conduction dominates at high temperatures for  $T > 200$  K. We compared the activation energy values from the plateaus observed on samples with  $8\%$  and  $9\%$  of Eu with the calculated values for transitions between the valence band and the  $4f$  level and found very good agreement. In addition, we verified that the saturation/reduction of the electrical resistances at low temperatures observed for samples with  $4\%$ ,  $5\%$ , and  $8\%$  is related to the relation between the activation and the thermal energy. We observed that when the activation energy becomes lower than the thermal energy as the temperature decreases bellow 40 K, there is a decreasing of the electrical resistance indicating that hole carriers could be thermally activated from a region of localized states to a region of delocalized states leading to a reduction of electrical resistance. The description of the conduction mechanisms of  $p$ -type  $\text{Pb}_{1-x}\text{Eu}_x\text{Te}$  alloys can lead to the improvement of the application of this compound on electrical and optical devices as well as in  $\text{PbTe}/\text{Pb}_{1-x}\text{Eu}_x\text{Te}$  nanostructures for spintronic devices.

#### ACKNOWLEDGMENTS

The authors would like to acknowledge CNPq, CAPES, and FAPEMIG for financial support.

- <sup>1</sup>G. Springholz, T. Schwarzl, W. Heiss, T. Fromherz, G. Bauer, M. Aigle, H. Pascherb, and I. Vavra, *Physica E* **13**, 876 (2002).
- <sup>2</sup>M. Böberl, T. Fromherz, J. Roither, G. Pillwein, G. Springholz, and W. Heiss *Appl. Phys. Lett.* **88**, 041105 (2006).
- <sup>3</sup>J. A. H. Coaquira, V. A. Chitta, N. F. Oliveira, Jr., P. H. O. Rappl, A. Y. Ueta, E. Abramof, and G. Bauer, *J. Supercond.* **16**, 115 (2003).
- <sup>4</sup>A. Prinz, G. Bauer, and G. Ihninger, *J. Cryst. Growth* **127**, 302 (1993).
- <sup>5</sup>M. Iida, T. Shimizu, H. Enomoto, and H. Ozaki, *Jpn. J. Appl. Phys., Part 1* **32**, 4449 (1993).
- <sup>6</sup>H. Krenn, W. Herbst, H. Pascher, Y. Ueta, G. Springholz, and G. Bauer, *Phys. Rev. B* **60**, 8117 (1999).
- <sup>7</sup>R. M. Rubinger, G. M. Ribeiro, A. G. de Oliveira, H. A. Albuquerque, R. L. da Silva, C. P. L. Rubinger, W. N. Rodrigues, and M. V. B. Moreira, *Semicond. Sci. Technol.* **21**, 1681 (2006).
- <sup>8</sup>S. Murakami, N. Nagaosa, and S.-C. Zhang, *Phys. Rev. Lett.* **93**, 156804 (2004).
- <sup>9</sup>G. Grabecki, *J. Appl. Phys.* **101**, 081722 (2007).
- <sup>10</sup>G. Springholz, A. Y. Ueta, N. Frank, and G. Bauer, *Appl. Phys. Lett.* **69**, 2822 (1996).
- <sup>11</sup>B. I. Shklovskii and A. L. Efros, *Electronic Properties of Doped Semiconductors*, Springer Series in Solid-State Sciences Vol. 45 (Springer-Verlag, Berlin, 1984).
- <sup>12</sup>S. Yuan, H. Krenn, G. Springholz, A. Y. Ueta, G. Bauer, and P. J. McCann, *Phys. Rev. B* **55**, 4607 (1997).